Am J Cancer Res 2026;16(6):2534-2547
www.ajcr.us /ISSN:2156-6976/ajcr0173430

Original Article

Reactive oxygen species-dependent regulation of hypoxia-inducible factor 1α/C-X-C motif chemokine receptor 4 signaling promotes ozone-induced cancer metastasis

Che-Hsin Lee[1,2,3,4], Chun-Sheng Chuang[1], Po-Yen Chiu[1], Pei-Hsuan Chen[1], Li-Hsien Wu[1], Ming-Der Huang[1], Chia C Wang[2,5]

[1]Department of Biological Sciences, National Sun Yat-sen University, Kaohsiung 80424, Taiwan; [2]Aerosol Science Research Center, National Sun Yat-sen University, Kaohsiung 80424, Taiwan; [3]Department of Medical Research, China Medical University Hospital, China Medical University, Taichung 40433, Taiwan; [4]Department of Medical Laboratory Science and Biotechnology, Kaohsiung Medical University, Kaohsiung 80708, Taiwan; [5]Department of Chemistry, National Sun Yat-sen University, Kaohsiung 80424, Taiwan

Received April 20, 2026; Accepted June 10, 2026; Epub June 15, 2026; Published June 30, 2026

Abstract: Air pollutants, including vehicle emissions and photochemical smog such as ozone, have become a significant health concern in most industrialized nations. Inhaling ozone has repeatedly been linked to increased lung inflammation, immune responses, and cancer development, ultimately speeding up lung cancer metastasis and leading to higher death rates. However, the direct connection between ozone exposure and tumor cell migration has not yet been definitively established. This study aims to investigate the effects of ozone exposure on cancer spread and its underlying mechanisms, focusing on the hypoxia-inducible factor 1α (HIF-1α)/C-X-C motif chemokine receptor 4 (CXCR4) pathway, which influences cancer cell migration and epithelial-mesenchymal transition (EMT). Using B16F10 melanoma and LL2 Lewis lung carcinoma cells, we examined how 1 ppm ozone exposure affects reactive oxygen species (ROS) production and its subsequent impact on the HIF-1α/CXCR4 pathway. Our results show a significant increase in HIF-1α/CXCR4 expression and EMT-related proteins after ozone exposure. Additionally, the use of arbutin, a known ROS scavenger, significantly reduced HIF-1α/CXCR4 levels and cell migration, confirming the role of ROS in ozone-induced metastasis. In summary, our research suggests that ozone promotes cancer spread by activating the HIF-1α/CXCR4 signaling pathway, highlighting an environmental factor that could facilitate cancer progression.

Keywords: Ozone, metastasis, hypoxia-inducible factor 1α, C-X-C motif chemokine receptor 4, epithelial-mesenchymal transition

Introduction

Air pollution has long been recognized as a major health problem in industrialized countries, dating back to the Industrial Revolution. Air pollutants originate from urban development, vehicle emissions, and municipal waste. Prolonged exposure to these pollutants has been linked to a wide range of diseases, including strokes, chronic obstructive pulmonary disease (COPD), heart disease, and lung cancer [1]. Despite increased environmental awareness and stricter emission standards, air pollution remains a serious concern. According to the World Health Organization (WHO) air quality report, 99% of the world's population lives in areas with poor air quality, resulting in about 4.2 million premature deaths worldwide from ambient air pollution.

Ozone, a primary pollutant classified as a reactive oxygen species (ROS), is primarily generated in photochemical smog via ultraviolet (UV) radiation. Inhaling ozone has been associated with acute damage to the airway epithelium, protein leakage, and the release of pro-inflammatory cytokines [2]. Recent research has examined the effects of ozone on respiratory neutrophilic inflammation and its potential role in promoting cancer metastasis. Ozone exposure

accelerates early tumor metastasis to the lungs by increasing neutrophil extracellular trap (NET) formation, which facilitates tumor cell colonization of lung tissues [3]. Epithelial-mesenchymal transition (EMT) is a vital process that promotes tumor metastasis. EMT is a biological process in which epithelial cells acquire a mesenchymal phenotype, leading to increased mobility, invasiveness, and resistance to apoptosis. A key characteristic of EMT is the elevated expression of N-cadherin and the reduced expression of E-cadherin, along with the activation of various transcription factors and signaling pathways [4].

Hypoxia-inducible factor-1 (HIF-1) is a heterodimeric transcription factor composed of α and β subunits that regulates critical processes in tumor growth, including metabolic reprogramming, angiogenesis, and cancer cell dissemination [5]. HIF-1α levels rise under low oxygen conditions or oxidative stress due to inhibition of prolyl hydroxylases (PHDs) [6]. The C-X-C motif chemokine receptor 4 (CXCR4), which is specifically activated by stromal-derived factor-1 (SDF-1), is closely associated with HIF-1 expression and regulation [7, 8]. Additionally, the SDF-1/CXCR4 pathway has been implicated in inducing EMT, supporting tumor invasion and migration in highly metastatic cancer cells [9, 10].

Despite existing evidence, the direct link between ozone exposure and tumor metastasis remains unclear. Tumor-intrinsic mechanism independent of immune priming *in vitro*, while the *in vivo* metastatic outcome may also be influenced by host microenvironmental factors. In this study, we aimed to determine whether ozone exposure alone, without immune system involvement, is sufficient to increase tumor cell metastasis. Using a controlled ozone exposure system, we exposed B16F10 melanoma and LL2 lung carcinoma cells to 1 ppm ozone, a concentration known to elicit measurable responses in cancer cells [11]. Previous animal studies have shown that 1 ppm ozone can cause significant biological damage, making it a key concentration for mechanistic research. Tian et al. reported that 1 ppm ozone exposure in female mice caused notable lung injuries and highlighted the role of the gut and lung microbiota in mediating these effects [12]. Prenatal ozone exposure also led to abnormal liver lipid metabolism in adult offspring, suggesting that 1 ppm can affect long-term metabolic outcomes [13]. Additionally, ozone (1 ppm) triggered prediabetic symptoms through changes in glycogen metabolism and insulin resistance [14]. Notably, occupational studies recorded instantaneous ozone levels ranging from 0.07 to 2.2 ppm in welding fumes, confirming that 1 ppm is a realistic peak level in specific environments [15]. Overall, these findings support the use of 1 ppm ozone in cell experiments as a relevant dose that reflects toxicological thresholds observed in animal studies and likely exposure levels in occupational settings.

Our results showed a significant increase in the HIF-1α/CXCR4 axis, as confirmed by Western blot analysis. Additionally, EMT-related changes were observed in both cell migration and invasion assays and in protein expression studies. Furthermore, *in vivo* experiments with ozone-treated tumor cells supported our findings. Understanding how ozone influences the HIF-1α/CXCR4 signaling pathway may help identify an environmental factor that promotes metastasis and affects cancer progression. These results highlight the importance of strategies to reduce ozone exposure, especially for at-risk cancer patients, to lower the risk of metastasis and improve clinical outcomes.

Materials and methods

Cells and reagents

B16F10 and LL2 cells were cultured in DMEM supplemented with 10% heat-inactivated fetal bovine serum (FBS), 1% glutamine, and 1% penicillin/streptomycin solution (100 units/mL penicillin and 100 μg/mL streptomycin) in 10 cm culture dishes. The dishes were incubated at 37°C with 5% CO_2, and the medium was replaced every 2 days until the cells reached approximately 80% confluence. LL2 cells were selected because lung tumors are directly relevant to inhaled ozone exposure. B16F10 melanoma cells were included as a highly metastatic model to examine whether ozone-induced oxidative stress can enhance metastatic phenotypes beyond respiratory-origin cancer cells. In addition, because the skin may be directly exposed to ambient ozone, B16F10 melanoma cells may also serve as a relevant skin-associated tumor model to evaluate whether ozone-derived ROS can exacerbate melanoma cell migration and metastatic potential. We clarified that direct physiological ozone exposure is

most relevant to respiratory tract and lung-associated cells, whereas the B16F10 model should be interpreted as both a highly metastatic melanoma model and a mechanistic model of ROS-mediated enhancement of metastatic behavior. Stromal cell-derived factor-1 (SDF-1), arbutin, and cobalt chloride hexahydrate ($CoCl_2$) were purchased from Sigma-Aldrich (Sigma-Aldrich, St. Louis, MO, USA). The HIF-1α inhibitor (SYP-5) was purchased from MedChemExpress (MedChemExpress LLC, Monmouth Junction, NJ, USA).

Ozone exposure and animal

In this model, the ozone exposure system consisted of two chambers driven by the ozone generator. The mixing chamber thoroughly combined ozone with artificial air to achieve a concentration of 1 ppm (± 0.2 ppm) and supplied ozone at a stable flow rate (below the maximum pressure of 10 mmHg; 4 liters/min) to cells in the exposure chamber (48 liters) (Supplementary Figure 1). The 6-well plates, containing 2 mL of fresh medium, were divided into ozone-treated and air-controlled groups and transferred into the exposure chamber. All plates were sealed with Parafilm during transfer, both before and after ozone exposure. Cells were exposed to ozone (1 ppm, 3 hours/day) or artificial air for three consecutive days. Ozone concentration was continuously monitored using a spectrometer and AvaSoft 8 software to ensure a consistent supply of ozone. In this exposure system, cells continued to proliferate after 3 days of culture under air or ozone exposure, which is the maximum duration for collecting experimental data from cultured cells. Female C 57 BL/6 mice were obtained from the National Laboratory Animal Center. Animal studies were approved by the Laboratory Animal Care and Use Committee of the National Sun Yat-sen University (permit number: 11226). Tumor cells (1×10^5) in 100 μL of medium were treated with ozone or left untreated. These cells were then injected into mice aged 6 weeks or older via the tail vein (n = 5). Based on our previous experience, the two cell lines exhibit different growth rates *in vivo* [16]. Mice injected with the B16F10 and LL2 cell lines were sacrificed on days 20 and 40, respectively. Lung weights were recorded, and metastatic tumor nodules were counted and used for Western blot analysis. The lungs were fixed with 4% paraformaldehyde for tissue section preparation. Tissue sections were stained with H & E and examined under 100× magnification for tumor nodules or metastases. Finally, lung tissue sections underwent immunohistochemical staining with anti-N-cadherin (Dilution: 1:100) (iREAL, Hsinchu, Taiwan), anti-E-cadherin (Dilution: 1:100) (Invitrogen, Carlsbad, CA, USA), anti-MMP-2 (GeneTex, Inc., CA, USA), and anti-SNAIL (Dilution: 1:100) (Invitrogen) antibodies. Each immunohistochemical (IHC) marker was evaluated at 400× magnification.

Western blot analysis

Ozone and arbutin affected protein expression in B16F10 and LL2 cells. B16F10 and LL2 cells (5×10^5 cells/well) were plated in 6-well plates and incubated at 37°C for 24 hours. After treating with arbutin (1.56 μM) for 6 hours, protein levels were measured by Western blotting. To determine protein concentrations, we used the Bicinchoninic Acid (BCA) Protein Assay kit (Pierce Biotechnology, Rockford, IL, USA). Proteins were separated by SDS-PAGE and then transferred to a PVDF membrane (Pall Life Sciences, Glen Cove, NY, USA). The membrane was incubated with primary antibodies: Proliferating Cell Nuclear Antigen (PCNA) (1:1000 dilution) (GeneTex), CXCR4 (1:1000) (GeneTex), HIF-1α (1:200) (Santa Cruz Biotechnology Inc, Santa Cruz, CA, USA), P-AKT (1:1000) (Santa Cruz Biotechnology), AKT (1:1000) (Santa Cruz Biotechnology), E-Cadherin (1:1000) (iREAL, Hsinchu, Taiwan), N-Cadherin (1:1000) (Invitrogen), MMP-2 (GeneTex), SNAIL (1:1000) (Santa Cruz Biotechnology Inc), and a monoclonal anti-β-actin antibody (1:10000) (Sigma-Aldrich). Secondary detection was performed using horseradish peroxidase-conjugated anti-mouse, anti-rabbit, or anti-goat IgG antibodies (1:20000) (Jackson ImmunoResearch Inc., West Grove, PA, USA). Protein-antibody complexes were visualized using an enhanced chemiluminescence system (T-Pro Biotechnology, New Taipei City, Taiwan). Signal quantification was performed using ImageJ [17].

Cell viability assay

Cell proliferation was evaluated using the WST-1 Cell Proliferation Assay Kit (Sigma-Aldrich) following the manufacturer's instructions, with absorbance measured at specific times using the SPECTROstar Nano Microplate Reader. The kit was employed to determine whether ozone-

promoted or arbutin-inhibited cell proliferation rates were affected by ozone. Cells were seeded in 96-well plates and exposed to ozone under different conditions for 3 days. Afterward, 100 μL of WST-1 reagent (diluted tenfold) was added, and samples were incubated at room temperature in the dark for 15 minutes. The optical density of the cell samples was then measured and recorded using the microplate reader.

Cell migration and invasion assay

The wound-healing assay was performed using ibidi 2-well culture inserts. The inserts were initially placed in 12-well plates. About 70 μL of cell suspension at 3×10^5 cells/mL was added to each well of the inserts. The plates were incubated overnight. Subsequently, the media and inserts were removed, and cells were supplied with either serum-free DMEM or fresh medium for 24 hours. Photomicrographs were taken at 0 and 24 hours after ozone exposure using an inverted microscope at 100× magnification. The wound gap was measured three times (upper, middle, and lower) in each well at both time points. The Transwell assay used Millicell Hanging Cell Culture Inserts with an 8.0 μm pore membrane. For the invasion assay, the inserts were coated with Matrigel and incubated at 37°C for 30 minutes to 1 hour to solidify. Cells were pretreated with a gossypol solution in 6-well plates for 24 hours, then trypsinized, resuspended, and diluted in DMEM to a final concentration of 2×10^5 cells/mL. The inserts were placed into 24-well plates and seeded with 200 μL of cell suspension in the upper chamber of each insert. Then, 500 μL of FBS-DMEM (containing either arbutin or DMSO) was carefully added to the basolateral side of each well. The plates were incubated for 24 hours. Afterward, the inserts were removed, rinsed twice with PBS, and immediately fixed with 4% paraformaldehyde for 5 minutes. DAPI staining was performed with a 1 μg/mL solution for 2 minutes in the dark. Finally, the migrated cells were counted under a fluorescence microscope at 200× magnification [18].

Total ROS assay

The ROS content assay was performed using the ROS-ID Total ROS Detection Kit (Enzo, Farmingdale, NY, USA) to evaluate trends in ROS levels after ozone exposure. Both cell types were seeded into 6-well culture plates at a density of 2×10^5 cells per mL and incubated overnight. The ROS assay stain stock solution was then diluted and thoroughly mixed with FBS-free medium to label the cells. Each well was suspended in 2 mL of FBS-free medium containing 1× stain stock and incubated for 60 minutes at 37°C, then exposed to ozone or air for 3 hours. After exposure, the treated cells were trypsinized and analyzed on the Attune N×T Acoustic Focusing Cytometer in the FITC channel (488-520 nm). Additionally, the dichlorodihydrofluorescein diacetate (DCFH-DA) assay (ChekineTM reactive oxygen species detection fluorometric assay) was used as a cell-based method to detect and quantify intracellular ROS, markers of cellular oxidative stress. This assay produces a fluorescent compound that emits green light at approximately 530 nm upon excitation at around 485 nm, and the green fluorescence was measured using a fluorescence plate reader.

Statistical analysis

The Student's t-test was used to assess the statistical significance of data collected from two-group experiments. SigmaPlot 10 displayed all statistical results and graphs. The Western blot protein expression graphs were analyzed using ImageJ, which comes bundled with Zulu OpenJDK 13.0.6.

Results

Ozone exposure promotes tumor progression

Ozone forms when ionized oxygen atoms recombine with un-ionized molecular oxygen. As a strong oxidant, ozone induces ROS generation in tissues. To assess the effect of ozone exposure on ROS production in tumor cells, we exposed two tumor cell lines (B16F10 and LL2) to 1 ppm ozone for 3 hours. Flow cytometry combined with the total ROS assay showed a significant increase in intracellular ROS levels in both tumor cell types after ozone exposure (*$P < 0.05$) (**Figure 1A**). We also used DCFDA to measure ROS levels in cells exposed to ozone (**Figure 1B**, **1C**) (***$P < 0.001$). Similar results were observed across different assays. To determine whether ozone exposure negatively affects cell viability, we subjected both cell lines to daily ozone exposure. The WST-1 assay indicated that ozone at this concentration was

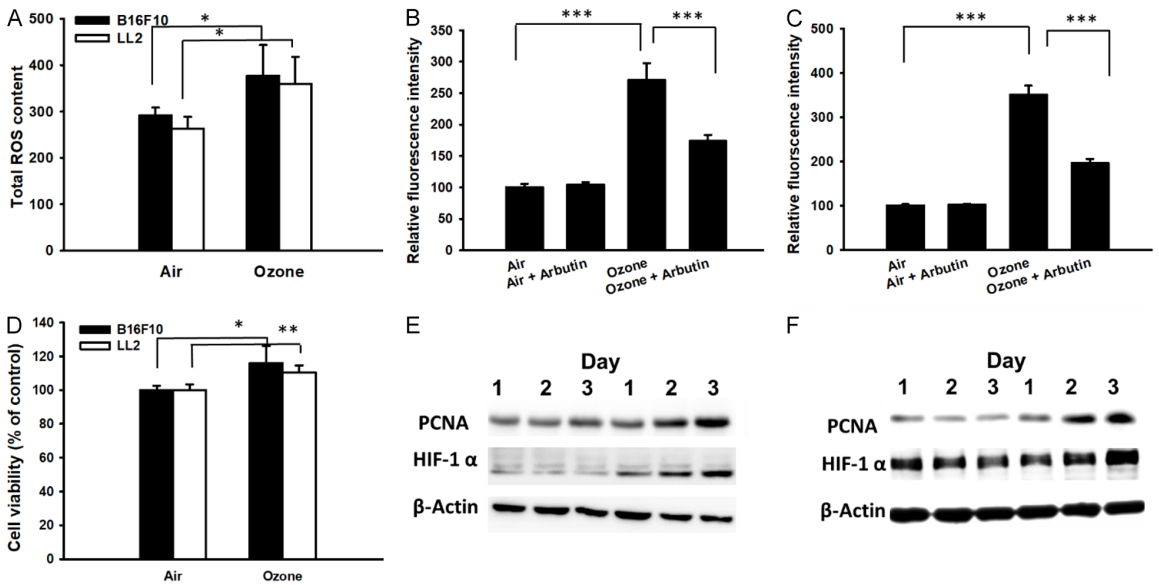

Figure 1. The effect of ozone exposure on tumor cells was studied by measuring ROS levels in B16F10 melanoma and LL2 lung carcinoma cells. (A) The ROS content was assessed using the ROS-ID Total ROS Detection Kit. Data from the 520 nm fluorescence indicates increased ROS levels. The increase in ROS in (B) B16F10 melanoma and (C) LL2 lung carcinoma cells was observed after three days of treatment with air or ozone, with or without arbutin (1.56 μM). These measurements were performed using the Chekine™ reactive oxygen species detection fluorometric assay. (D) Cell proliferation of B16F10 melanoma and LL2 lung carcinoma was evaluated following three-day ozone exposure, revealing enhanced proliferation in both cell lines. Results are shown as mean ± SD with a sample size of 6; statistical significance is indicated by *P < 0.05, **P < 0.01, and ***P < 0.001. Western blot images display the expression of PCNA and HIF-1α proteins in (E) B16F10 (F) LL2 cells exposed to ozone or air at various time points.

not harmful and actually promoted tumor cell proliferation compared with the air-exposed control group (*P < 0.05; **P < 0.01) (**Figure 1D**). Western blot analysis of PCNA and HIF-1α expression showed increased protein levels in ozone-exposed cells (**Figure 1E**, **1F**). PCNA was measured to assess whether ozone exposure affects proliferative activity under the same exposure conditions. Exposure to 1 ppm ozone for three hours daily can induce subtle changes, but exposure over 3 consecutive days produces more noticeable and detectable physiological responses. The effects of ozone on cells were consistent in this exposure system. These findings suggest that ozone induces ROS production and promotes tumor cell proliferation.

Ozone exposure enhances tumor cell migration

Since ozone promotes tumor cell proliferation, we next investigated whether it also affects tumor metastasis. The wound-healing migration assay showed that both tumor cell lines exhibited significantly increased migration distances after 3 hours of ozone exposure, indicating enhanced cell motility. These findings were supported by microscopy images (**Figure 2A**) and corresponding bar charts (**Figure 2B**) (***P < 0.001). Removing cells might facilitate wound healing by promoting cell proliferation. The Transwell assay was performed to verify that ozone can stimulate cell migration. The effect of one-day ozone exposure on cell proliferation was not evident (**Figure 1E**, **1F**). Additionally, a 24-hour Transwell migration assay was conducted to confirm these results. The data showed that the number of migrated cells was significantly higher in the ozone-treated groups compared to the air-exposed control groups. To determine whether the increase in migration was influenced by CXCR4 signaling, we added the SDF-1 chemokine to the assay. The results indicated increased migration with SDF-1 addition (**Figure 2C**, **2D**). Ozone enhances cell migration, and this effect is more pronounced when SDF-1 is added (**Figure 2E**, **2F**). The binding of tumor cells to SDF-1 induces AKT activation and increases PCNA expression (Supplementary Figure 2).

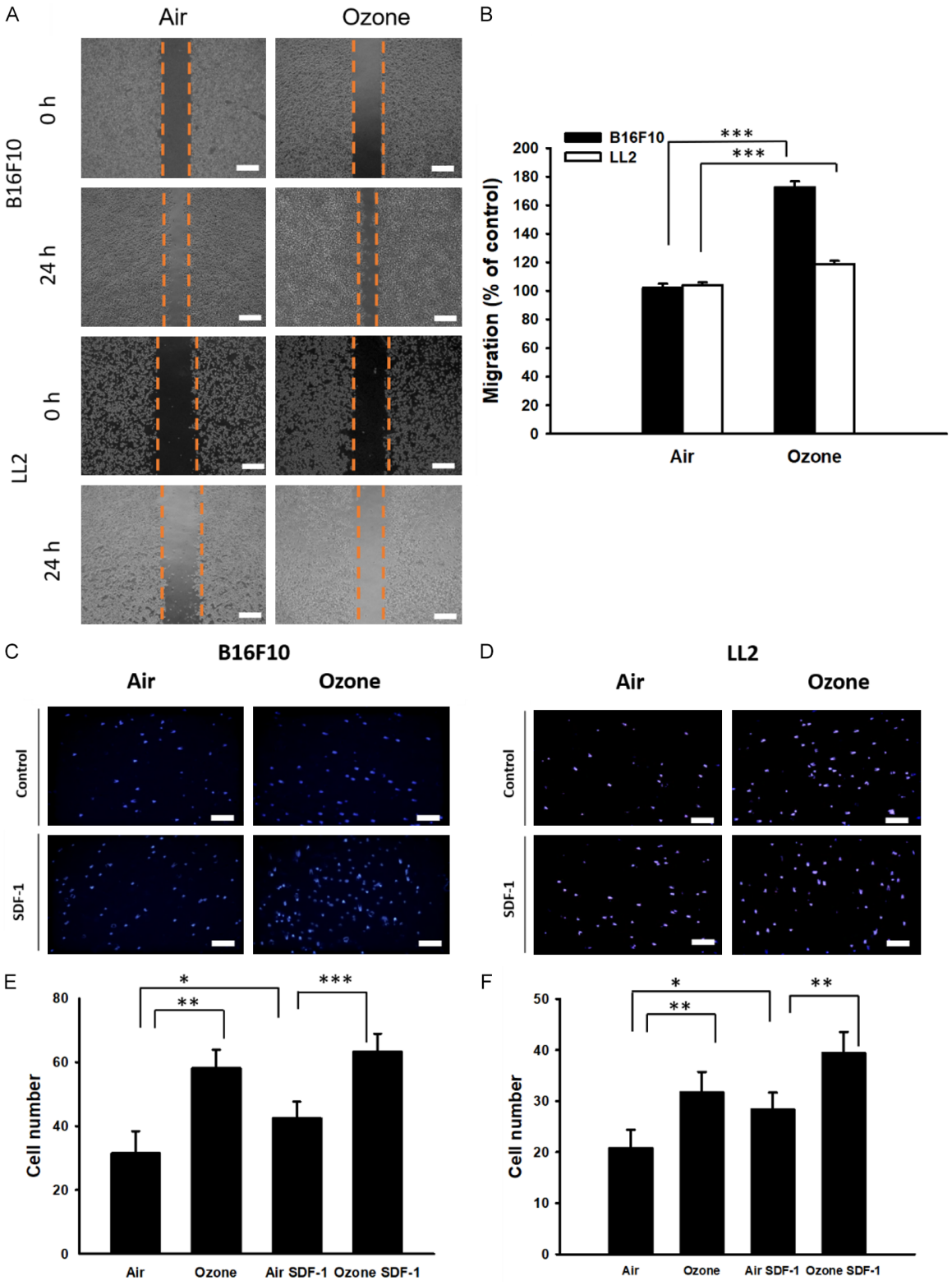

Figure 2. The cell migration ability of B16F10 and LL2 cells after ozone exposure was examined. Wound-healing assays were performed with either air or 1 ppm ozone exposure for 3 hours. Gap closure was measured and photographed (100× magnification) at 0 and 24 hours after exposure began. The migration distances of (A) B16F10 and LL2 cells were measured at 0 and 24 hours (×200), and the results are shown in (B). The effects of ozone on cellular migration in B16F10 and LL2 cells were evaluated. B16F10 and LL2 cells treated with ozone exposure and SDF-1 induction were analyzed using *in vitro* Transwell assays. The number of cells treated with either ozone or

SDF-1 was measured. (C, E) B16F10 and (D, F) LL2 cells were transferred to 24-well plates for a 3-hour exposure. Both the air and ozone groups received either control or SDF-1-containing media to assess migration support. The number of cells treated with ozone exposure and SDF-1 were quantified. The (E) B16F10 and (F) LL2 cell counts were calculated and visualized using a fluorescence microscope (×200) 24 hours after exposure (n = 6; mean ± SD; ***P < 0.001). Scale bar = 50 μm (×200).

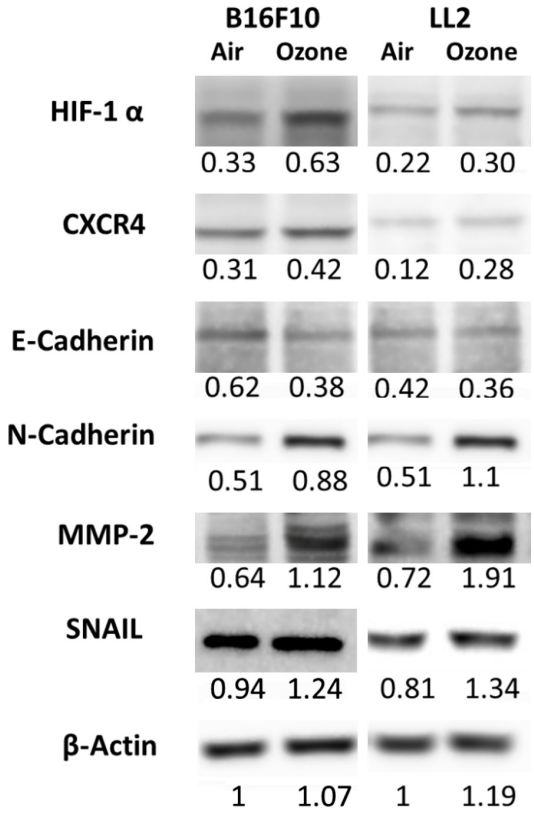

Figure 3. The effects of ozone on the HIF-1α/CXCR4 pathway and EMT markers in B16F10 and LL2 *in vitro* models. Western blot images showing levels of HIF-1α, CXCR4, E-cadherin, N-cadherin, MMP-2, and SNAIL proteins. Inset values represent protein expression levels normalized to β-Actin.

Ozone enhances HIF-1α/CXCR4 axis expression and EMT activity

We used $CoCl_2$ to stabilize HIF-1α [6] and confirmed that CXCR4 expression was indeed increased (Supplementary Figure 3A). Elevated CXCR4 due to ozone exposure was inhibited by inhibitors of HIF-1α (SYP-5) [19]. Inhibition of HIF-1α (SYP-5 as HIF-1α inhibitor) resulted in decreased downstream CXCR4 levels (Supplementary Figure 3A). Ozone-exposed B16F10 and LL2 cells were treated with SYP-5, followed by Transwell analysis. SYP-5 treatment significantly reduced ozone-enhanced tumor cell migration, supporting the conclusion that HIF-1α contributes functionally to ozone-induced migratory activity (Supplementary Figure 3B, 3C). The HIF-1α/CXCR4 axis exists. Furthermore, to investigate whether ozone-induced ROS affects the HIF-1α/CXCR4 pathway [7, 8], we conducted Western blot analysis. Our results showed that ozone exposure significantly increased HIF-1α and CXCR4 levels in both B16F10 and LL2 cell lines (**Figure 3**), suggesting a possible role in tumor metastasis. We also examined EMT markers and found a notable decrease in E-cadherin expression, indicating reduced epithelial cell polarity and weaker cell adhesion. While N-cadherin levels increased in both cell lines, the trend suggested upregulation after ozone exposure, consistent with its expected antagonistic relationship with E-cadherin (**Figure 3**). The other EMT markers (MMP-2, SNAIL) were similarly increased by ozone. To confirm that these effects depended on ROS, we added 1.56 μM arbutin, a known ROS scavenger (**Figure 1B**, **1C**) [20], to counteract ozone-generated ROS [20]. Western blot analysis showed that arbutin treatment significantly decreased HIF-1α levels in B16F10 melanoma cells. Additionally, CXCR4 expression was notably reduced after arbutin treatment in both air- and ozone-exposed groups (**Figure 4A**). Similar effects were observed in LL2 cells, confirming that arbutin suppresses the HIF-1α/CXCR4 axis (**Figure 4B**). Regarding EMT regulation, arbutin effectively reduced ozone-induced N-cadherin upregulation and restored E-cadherin, MMP-2, and SNAIL levels (**Figure 4**). To assess ozone's impact on tumor migration further, we performed a migration assay with arbutin treatment. Results showed a significant reduction in migration rates for both tumor cell types after arbutin administration. These were visualized using fluorescence microscopy (**Figure 5A**, **5B**) and quantified with bar charts (*P < 0.05, **P < 0.01, ***P < 0.001) (**Figure 5C**, **5D**). The invasion assay showed a similar pattern (**Figure 5E**, **5F**); LL2 cells were less likely to breach the extracellular matrix compared to B16F10 cells (**Figure 5G**, **5H**) (*P < 0.05, **P < 0.01, ***P < 0.001). These results confirm that arbutin effectively counteracts ozone-induced tumor cell migration and invasion.

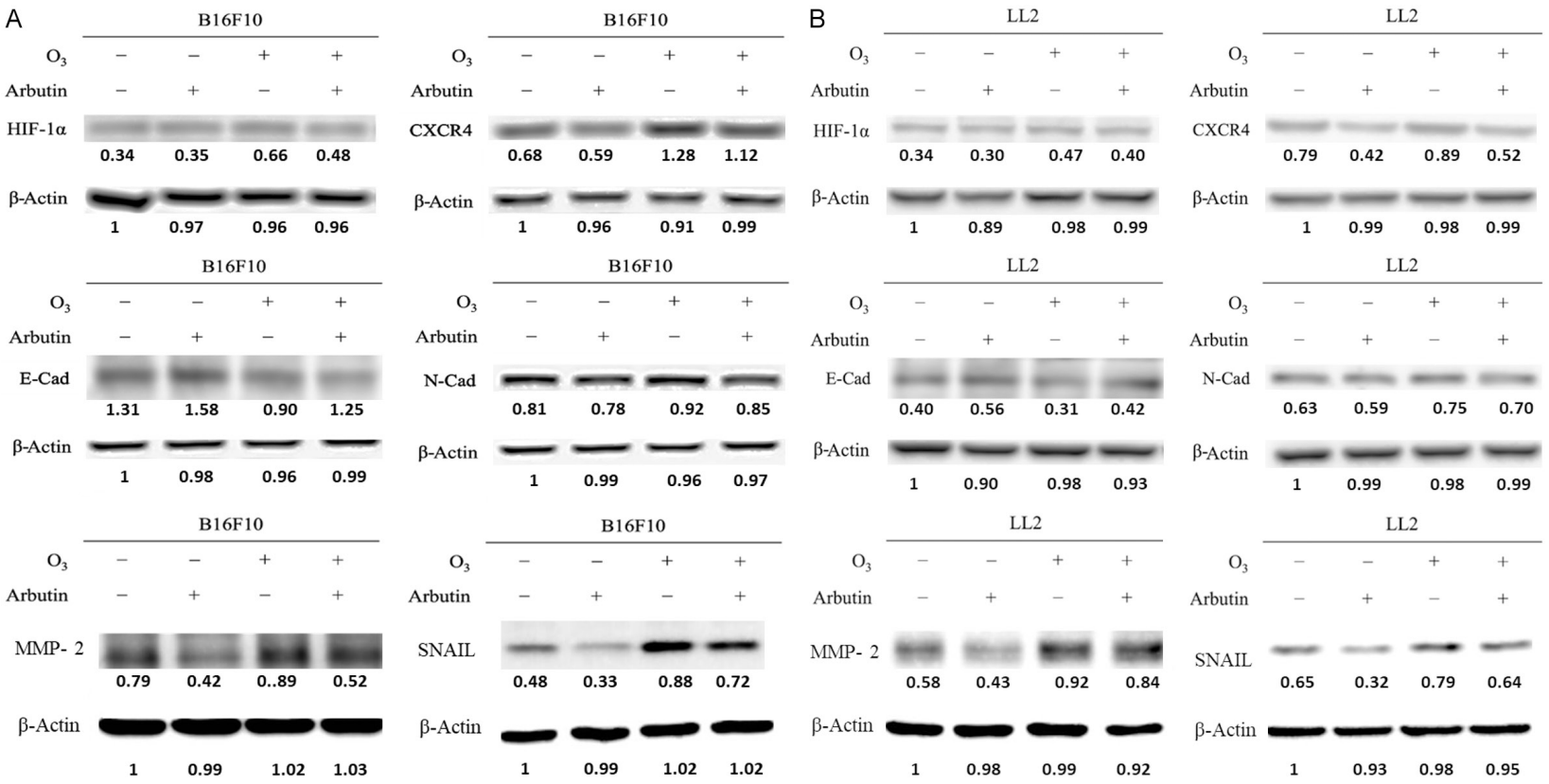

Figure 4. The ROS-related effects of *in vitro* arbutin application on ozone-exposed EMT depolarization and HIF-1α/CXCR4 pathway downregulation in (A) B16F10 and (B) LL2 cells. Protein expressions of HIF-1α, CXCR4, E-cadherin (E-Cad), N-cadherin (N-Cad), MMP-2, and SNAIL are shown with arbutin-reversal treatment. Inset values indicate protein levels normalized to β-Actin. Each experiment was repeated three times with similar results.

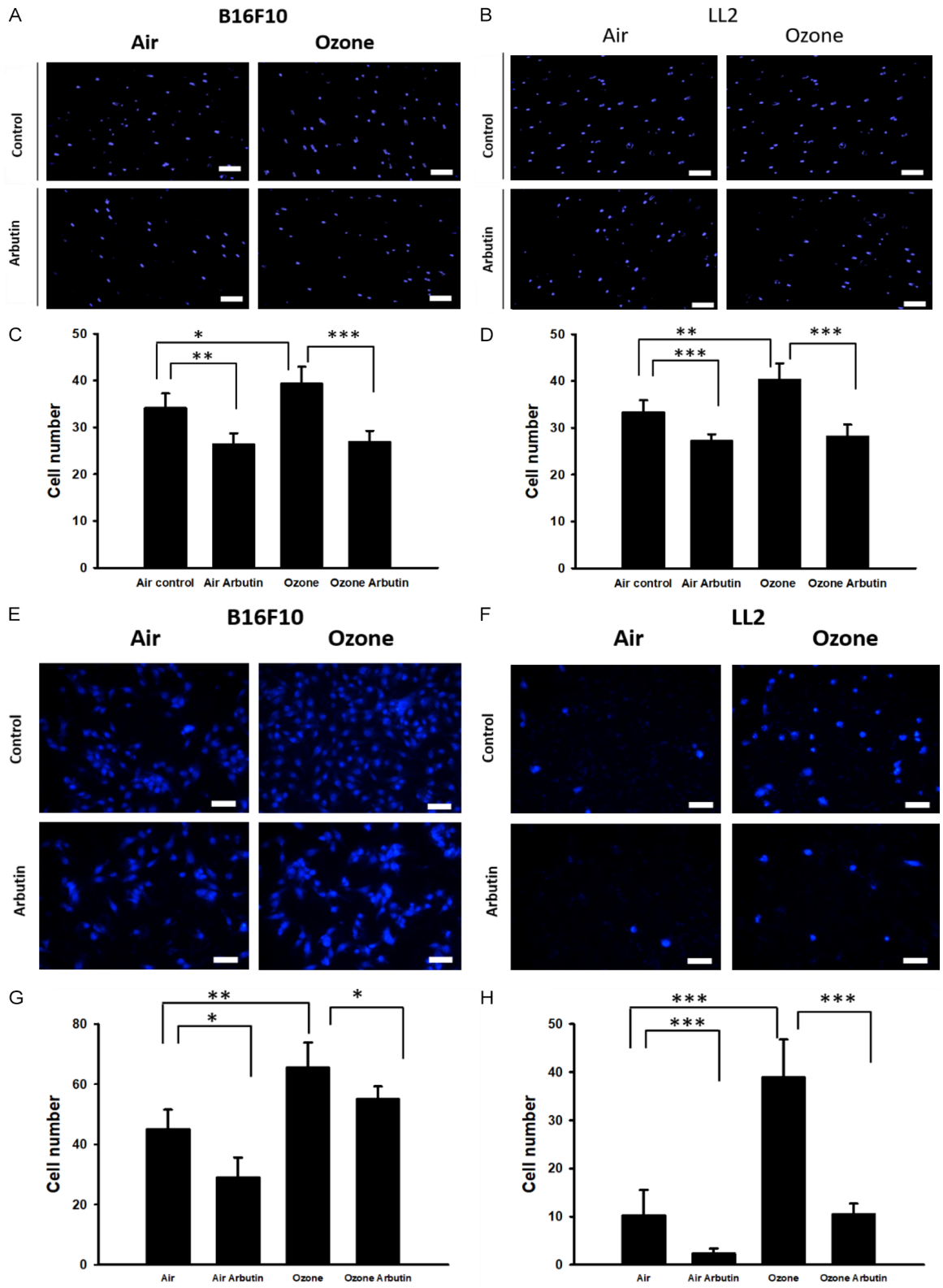

Figure 5. Transwell assays were used to detect the inhibitory effect of arbutin on tumor cell migration after ozone treatment. (A, C) B16F10 and (B, D) LL2 cells were treated with arbutin (1.56 μM). B16F10 and LL2 cells were placed on the upper layer of Transwell and then treated with arbutin or ozone. The lower layer of Transwell was stained with DAPI, and (C) B16F10 cells and (D) LL2 cells were counted using a fluorescence microscope 24 hours after exposure began. Invasion assays were used to detect the inhibitory effect of arbutin on tumor cell invasion after ozone treatment. (E, G) B16F10 and (F, H) LL2 cells were treated with arbutin (1.56 μM). B16F10 and LL2

cells were placed on the upper layer of Transwell coated with Matrigel and then treated with arbutin or ozone. The lower layer of the Transwell was stained with DAPI, and (G) B16F10 cells and (H) LL2 cells were counted under a fluorescence microscope 24 hours after exposure began (n = 6; mean ± SD; *P < 0.05; **P < 0.01; ***P < 0.001). Scale bar = 50 μm (×200).

Ozone-exposed tumor cells exhibit higher metastatic potential in vivo

To assess whether ozone exposure promotes tumor metastasis *in vivo*, we used a mouse metastasis model [21]. After tail vein injection of ozone-pretreated B16F10 and LL2 cells, tumor nodules were significantly visible on the lung surface in the ozone-treated group (**Figure 6A**). Additionally, mice injected with ozone-treated cells showed notably higher lung weights compared to control groups (**P < 0.01) (**Figure 6B**). Histological analysis revealed that tumor nodules were much more prominent in the lungs of mice injected with ozone-treated cells compared to controls (**Figure 6C**). Conversely, mice injected with air-treated control cells had fewer and smaller metastatic colonies (**Figure 6D**). The increase in metastatic activity appears partly due to the upregulation of MMP-2 and SNAIL in the ozone-treated group, as demonstrated by IHC-stained lung tissue sections (**Figure 6E**). IHC staining also slightly indicated that this rise in metastatic activity could be partly attributed to the upregulation of MMP-2 and SNAIL, with a slight increase in N-cadherin expression in the ozone-treated group. Conversely, E-cadherin was significantly reduced in this group (**Figure 6E**). These results strongly suggest that short-term ozone exposure enhances tumor cell migration and metastasis, even after the cells are no longer exposed to ozone. Tumor-intrinsic mechanism under *in vitro* conditions, while *in vivo* metastasis may also involve host microenvironmental influences.

Discussion

Since the Industrial Revolution, air pollution has been a significant health issue in industrialized countries. Every year, about 4.2 million people worldwide, including 237,000 children, die from diseases related to air pollution [22]. The rapid growth of society and lifestyle changes have led to higher emissions of nitrogen oxides (NOx) and volatile organic compounds (VOCs) from vehicles and industries, resulting in ozone formation through photochemical reactions [23]. Both indoor and outdoor ozone concentrations are unknowingly inhaled daily, causing chronic and acute airway inflammation such as coughing, asthma, COPD, and even lung cancer [1]. People with preexisting lung conditions or lung cancer are especially vulnerable to ozone's harmful effects. Inhaling oxygen naturally generates ROS in the lungs, thereby increasing oxidative stress. Excess ROS can promote cancer cell growth, differentiation, and spread [24]. Our results show that ozone exposure significantly affects tumor activity. In this study, we used lung cancer (LL2) and melanoma (B16F10) cell lines, both susceptible to ozone, to explore how environmental air pollution impacts cancer progression. To examine the link between ozone exposure and ROS production, B16F10 and LL2 cells were exposed to ozone under controlled conditions and then tested with total ROS detection kits. The findings confirmed a notable increase in ROS levels in ozone-treated tumor cells compared with the control group (**Figure 1**). However, responses varied between tumor types and normal cells, likely due to inherent cellular differences, such as variations in ROS tolerance or reliance on alternative signaling pathways. Additionally, increased oxidative stress has been linked to the activation of the transcription factors HIF-1α and SNAIL (**Figures 3**, **4**), which regulate the EMT pathway, even in the absence of hypoxia [25]. EMT induction enhances cancer cell movement and promotes a more aggressive mesenchymal phenotype, ultimately driving tumor progression and worsening prognosis [26]. Our experiments, both in living organisms and in cell cultures, support this phenomenon. Morphological changes were observed during wound healing assays, where ozone-treated groups displayed greater migration and faster wound closure (**Figure 2**). Likewise, Transwell assays showed a significant increase in cell migration and invasion, with roughly 20% more tumor cells moving in the ozone-exposed group compared to air-treated controls (**Figure 2**). Moreover, images from an *in vivo* metastasis model revealed more tumor nodules and colonies on the lung surface after injecting ozone-pretreated tumor cells (**Figure 6**). These results

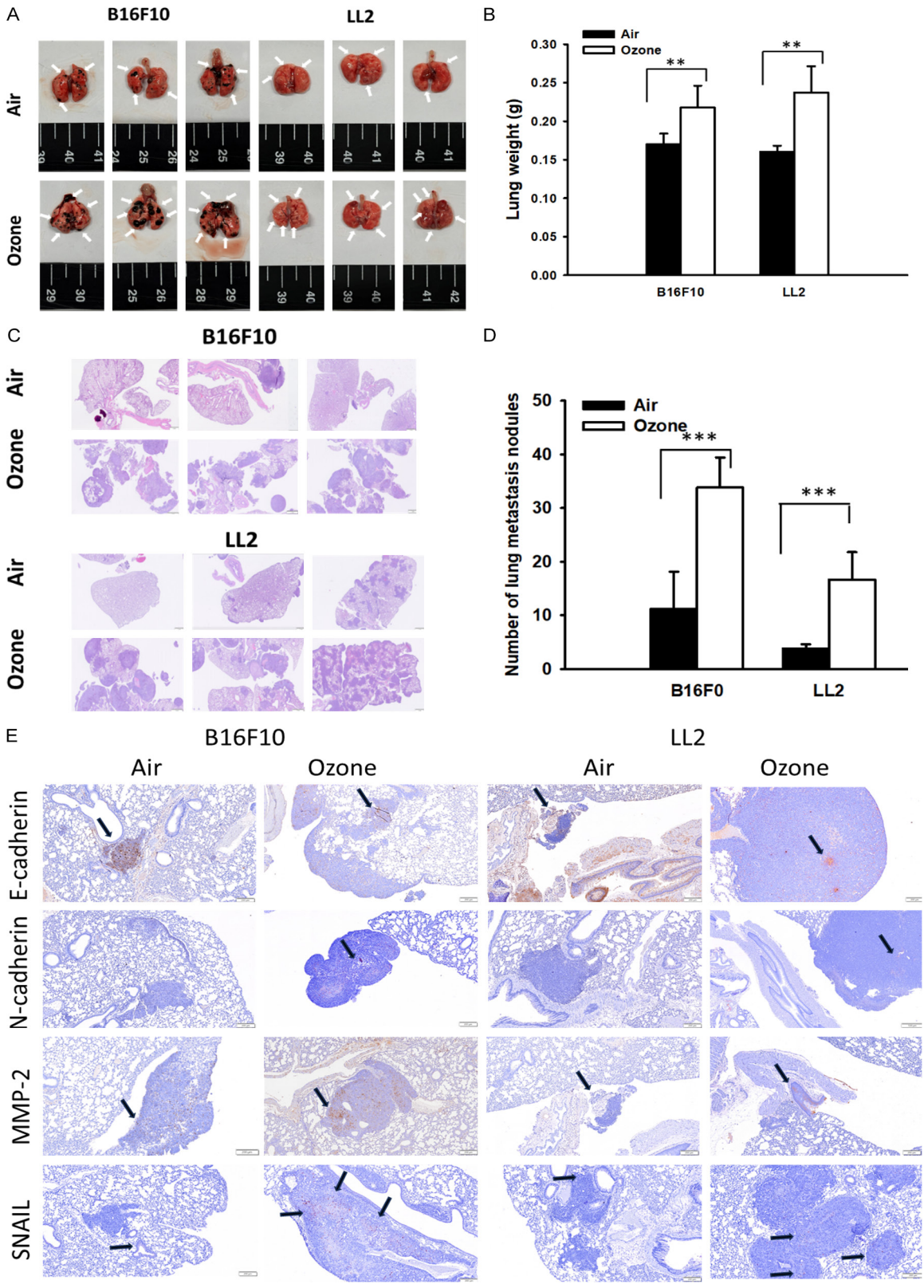

Figure 6. The effects of ozone on the B16F10 and LL2 tumor migration phenomena *in vivo*. The nodes of the lungs with visible metastatic growth were taken on day 20 for B16F10 and day 40 for LL2, respectively, after intravenous injection. (A) Macroscopic view of lung metastasis (n = 3). The white arrow points to tumor nodules. (B) Mice were sacrificed, and the lung tumor weights were measured (n = 5; mean ± SD; **P < 0.01). Histological examination of

pulmonary tumor nodules. Lung metastasis nodules were photographed (C) and further quantified (D) under a light microscope (×100). (E) Lung tissue excised and immunostained with antibodies against E-cadherin, N-cadherin, MMP2, and SNAIL (×400). Scale bar = 200 μm (×400). Black arrows point to positive signals.

suggest that short-term ozone exposure might have lasting effects on tumor progression, even after direct exposure stops.

ROS play a vital role in activating the HIF-1α pathway and multiple downstream signaling cascades, including EMT and CXCR4 modulation, both of which contribute to cancer cell growth and spread [7]. The ozone-induced increase in the HIF-1α/CXCR4 axis has been strongly linked to cancer progression in previous studies [27] and was also observed in our ozone-exposed cell samples (**Figures 3**, **4**). SDF-1 (CXCL12) is produced by multiple stromal and tissue-resident cells, including fibroblasts, endothelial cells, epithelial cells, bone marrow stromal cells, and lung-resident stromal cells [9, 27]. In the lung metastatic microenvironment, host-derived SDF-1 may provide chemotactic signals for CXCR4-expressing tumor cells. We also clarified that our study examined ozone-pretreated tumor cells rather than direct ozone exposure of host tissues; therefore, whether ozone exposure alters host SDF-1 production remains an important question for future studies. To further confirm the involvement of ROS in this pathway, we introduced arbutin, a well-known ROS scavenger [28]. Notably, arbutin treatment significantly lowered CXCR4 expression in B16F10 cells, indicating that ROS is a key mediator of ozone-induced tumor spread (**Figures 1**, **6**). Furthermore, arbutin administration effectively reduced the metastatic potential of ozone-induced tumor cells.

Inflammation plays a vital role in cancer progression [21]. In addition to its chemical irritant effects, ozone-induced ROS have been widely shown to damage lung epithelial cells, leading to the release of inflammatory mediators and increased vascular permeability [29]. This subsequently results in lung inflammation, often accompanied by neutrophil infiltration. Rocks et al. demonstrated that ozone exposure (2 ppm for 3 hours over 3 days) induces pulmonary neutrophilic inflammation and promotes the formation of neutrophil extracellular traps (NETs), which facilitate tumor metastasis to the lungs [3]. Lung inflammation caused by air pollutants or respiratory viral infections [30] can influence metastatic processes. Inflammation or immune cell infiltration can easily alter the lung microenvironment, making it more conducive to metastatic tumor cells. However, our study emphasizes that exposure to air pollutants, such as ozone, can trigger metastatic properties in tumor cells. Ozone reacts rapidly with extracellular and membrane-associated biomolecules, including lipids and proteins, generating secondary oxidation products such as lipid ozonation products and peroxides. These secondary mediators can disrupt redox homeostasis and promote intracellular ROS generation. This indicates that pollutant stimulation of organs prone to metastasis and primary tumors may lead to tumor spread. Not only can tumor metastasis be driven by inflammatory cells, but the cancer itself may also experience pressure that promotes metastasis.

Our findings, although based on murine models, have clear implications for human cancers. The HIF-1α/CXCR4 signaling axis, which we identified as a key mediator of ozone-induced migration, has been consistently associated with poor prognosis and metastatic spread across various human cancers, including non-small cell lung carcinoma, melanoma, and colorectal cancer. Elevated HIF-1α levels have been observed in human tumor biopsies and are associated with increased CXCR4 expression, which enhances chemokine-driven invasion and organ-targeted metastasis [31]. Additionally, EMT regulators such as SNAIL and MMPs, which were upregulated in our ozone-treated mouse cancer models, are well-established markers of aggressive cancers in humans and are associated with therapeutic resistance [32]. Furthermore, the role of reactive oxygen species in stabilizing HIF-1α has been documented in human cancer cell lines and clinical samples, where oxidative stress promotes tumor progression and metastasis [33]. Overall, these similarities suggest that the mechanisms we uncovered are not limited to experimental models and may also operate in human cancers. While further validation using patient-derived xenografts and clinical samples is necessary, the consistency of our results with human data emphasizes their potential

translational significance. It highlights the broader role of environmental pollutants, such as ozone, in worsening cancer aggressiveness. While it is widely accepted that ozone exposure contributes to lung cancer development, our data indicate that it also plays a significant role in the metastatic spread of both lung cancer and melanoma cells. Meanwhile, ozone also has a direct antitumor effect in some cancers. It also has indirect effects, such as immunomodulatory, synergistic, or adjuvant effects with various anticancer drugs and radiation [34]. From a personalized medicine perspective, environmental factors such as ozone exposure should be regarded as potential contributors to cancer progression, and patients should be advised accordingly. Despite efforts to improve air quality, targeted inhibition of prometastatic signaling pathways [33, 35] and localized inflammation may offer promising therapeutic strategies. Addressing these factors could improve patient prognosis and decrease cancer-related mortality.

Acknowledgements

Che-Hsin Lee and Chia C Wang acknowledge the support from the Aerosol Science Research Center, National Sun Yat-sen University, under the grant of “Higher Education Sprout Project - The Featured Areas Research Center Program”, Ministry of Education, Taiwan.

Disclosure of conflict of interest

None.

Address correspondence to: Dr. Che-Hsin Lee, Department of Biological Sciences, National Sun Yat-sen University, 70 Lienhai Road, Kaohsiung 80424, Taiwan. E-mail: chlee@mail.nsysu.edu.tw; Dr. Chia C Wang, Department of Chemistry, National Sun Yat-sen University, Kaohsiung 80424, Taiwan. E-mail: chiawang@mail.nsysu.edu.tw

References

[1] Lee YG, Lee PH, Choi SM, An MH and Jang AS. Effects of air pollutants on airway diseases. Int J Environ Res Public Health 2021; 18: 9905.

[2] Sokolowska M, Quesniaux VFJ, Akdis CA, Chung KF, Ryffel B and Togbe D. Acute respiratory barrier disruption by ozone exposure in mice. Front Immunol 2019; 10: 2169.

[3] Rocks N, Vanwinge C, Radermecker C, Blacher S, Gilles C, Marée R, Gillard A, Evrard B, Pequeux C, Marichal T, Noel A and Cataldo D. Ozone-primed neutrophils promote early steps of tumour cell metastasis to lungs by enhancing their NET production. Thorax 2019; 74: 768-779.

[4] Yen WC, Li QZ, Wu LH, Lee WY, Chang WW, Chien PJ and Lee CH. *Salmonella* inhibits tumor metastasis by downregulating epithelial cell adhesion molecules through the protein kinase-B/mammalian target of rapamycin signaling pathway. Int J Biol Macromol 2023; 253: 126913.

[5] Shiau AL, Shen YT, Hsieh JL, Wu CL and Lee CH. *Scutellaria barbata* inhibits angiogenesis through downregulation of HIF-1 α in lung tumor. Environ Toxicol 2014; 29: 363-370.

[6] Lee CH, Wu CL and Shiau AL. Hypoxia-induced cytosine deaminase gene expression for cancer therapy. Hum Gene Ther 2007; 18: 27-38.

[7] Guan G, Zhang Y, Lu Y, Liu L, Shi D, Wen Y, Yang L, Ma Q, Liu T, Zhu X, Qiu X and Zhou Y. The HIF-1α/CXCR4 pathway supports hypoxia-induced metastasis of human osteosarcoma cells. Cancer Lett 2015; 357: 254-264.

[8] Lee TH, Lin GY, Yang MH, Tyan YC and Lee CH. *Salmonella* reduces tumor metastasis by downregulation C-X-C chemokine receptor type 4. Int J Med Sci 2021; 18: 2835-2841.

[9] Tu Z, Xie S, Xiong M, Liu Y, Yang X, Tembo KM, Huang J, Hu W, Huang X, Pan S, Liu P, Altaf E, Kang G, Xiong J and Zhang Q. CXCR4 is involved in CD133-induced EMT in non-small cell lung cancer. Int J Oncol 2017; 50: 505-514.

[10] Duan Y, Zhang S, Wang L, Zhou X, He Q, Liu S, Yue K and Wang X. Targeted silencing of CXCR4 inhibits epithelial-mesenchymal transition in oral squamous cell carcinoma. Oncol Lett 2016; 12: 2055-2061.

[11] van Hoof HJ, Zijlstra FJ, Voss HP, Garrelds IM, Dormans JA, van Bree L and Bast A. The effect of ozone exposure on the release of eicosanoids in guinea-pig BAL fluid in relation to cellular damage and inflammation. Mediators Inflamm 1997; 6: 355-361.

[12] Tian Y, Xu P, Wu X, Gong Z, Yang X, Zhu H, Zhang J, Hu Y, Li G, Sang N and Yue H. Lung injuries induced by ozone exposure in female mice: potential roles of the gut and lung microbes. Environ Int 2024; 183: 108422.

[13] Yue H, Zhang J, Wu X, Tian Y, Liang X, Zhu H, Hu Y and Li B. Abnormal liver lipid metabolism in adult offspring induced by prenatal ozone exposure. J Hazard Mater 2025; 496: 139222.

[14] Tian Y, Wu X, Gong Z, Liang X, Zhu H, Zhang J, Hu Y, Li B, Xu P, Guo K and Yue H. Ozone exposure induces prediabetic symptoms through hepatic glycogen metabolism and insulin resistance. Toxics 2025; 13: 652.

[15] Park JH, Mudunkotuwa IA, Kim JS, Stanam A, Thorne PS, Grassian VH and Peters TM. Physicochemical characterization of simulated welding fume from a spark discharge system. Aerosol Sci Technol 2014; 47: 768-776.
[16] Liu CH, Weng JR, Wu LH, Song RY, Huang MD, Wu XH, Wang CC and Lee CH. Arbutin overcomes tumor immune tolerance by inhibiting tumor programmed cell death-ligand 1 expression. J Cancer 2024;15: 5308-5317.
[17] Wu PS, Weng JR, Chiu SH, Wu LH, Chen PH, Wang YX, Chiu PY and Lee CH. Hinokitiol reduces tumor metastasis by regulating epithelial cell adhesion molecule via protein kinase-B/mammalian target of rapamycin signaling pathway. Am J Cancer Res 2025; 15: 59-68.
[18] Wu LH, Huang YT, Lin CY and Lee CH. *Salmonella*-induced inhibition of β3-adrenoceptor expression in tumors and reduces tumor metastasis. J Cancer 2024; 15: 1203-1212.
[19] Xie Q, Wang J, Li R, Liu H, Zhong Y, Xu Q, Ge Y, Li C, Sun L and Zhu J. IL-6 signaling accelerates iron overload by upregulating DMT1 in endothelial cells to promote aortic dissection. Int J Biol Sci 2024; 20: 4222-4237.
[20] Wang L, Tian Y, Li L, Cai M, Zhou X, Su W, Hua X and Yuan X. Temporary alleviation of MAPK by arbutin alleviates oxidative damage in the retina and ARPE-19 cells. Heliyon 2024; 10: e32887.
[21] Chen MC, Chang WW, Kuan YD, Lin ST, Hsu HC and Lee CH. Resveratrol inhibits LPS-induced epithelial-mesenchymal transition in mouse melanoma model. Innate Immun 2012; 18: 685-93.
[22] Zhang JJ, Wei Y and Fang Z. Ozone pollution: a major health hazard worldwide. Front Immunol 2019; 10: 2518.
[23] Fan K, Dong N, Fang M, Xiang Z, Zheng L, Wang M, Shi Y, Tan G, Li C and Xue Y. Ozone exposure affects corneal epithelial fate by promoting mtDNA leakage and cGAS/STING activation. J Hazard Mater 2024; 465: 133219.
[24] Nakamura H and Takada K. Reactive oxygen species in cancer: current findings and future directions. Cancer Sci 2021; 112: 3945-3952.
[25] Xiong Y, Liu Y, Xiong W, Zhang L, Liu H, Du Y and Li N. Hypoxia-inducible factor 1 α-induced epithelial-mesenchymal transition of endometrial epithelial cells may contribute to the development of endometriosis. Hum Reprod 2016; 31: 1327-1338.
[26] Pangilinan CR, Wu LH and Lee CH. *Salmonella* impacts tumor-induced macrophage polarization, and inhibits SNAI1-mediated metastasis in melanoma. Cancers (Basel) 2021; 13: 2894.
[27] Taichman RS, Cooper C, Keller ET, Pienta KJ, Taichman NS and McCauley LK. Use of the stromal cell-derived factor-1/CXCR4 pathway in prostate cancer metastasis to bone. Cancer Res 2002; 62: 1832-1837.
[28] Polouliakh N, Ludwig V, Meguro A, Kawagoe T, Heeb O and Mizuki N. α-arbutin promotes wound healing by lowering ROS and upregulating insulin/IGF-1 pathway in human dermal fibroblast. Front Physiol 2020; 11: 586843.
[29] Stenfors N, Bosson J, Helleday R, Behndig AF, Pourazar J, Törnqvist H, Kelly FJ, Frew AJ, Sandström T, Mudway IS and Blomberg A. Ozone exposure enhances mast-cell inflammation in asthmatic airways despite inhaled corticosteroid therapy. Inhal Toxicol 2010; 22: 133-139.
[30] Chia SB, Johnson BJ, Hu J, Valença-Pereira F, Chadeau-Hyam M, Guntoro F, Montgomery H, Boorgula MP, Sreekanth V, Goodspeed A, Davenport B, De Dominici M, Zaberezhnyy V, Schleicher WE, Gao D, Cadar AN, Petriz-Otaño L, Papanicolaou M, Beheshti A, Baylin SB, Guarnieri JW, Wallace DC, Costello JC, Bartley JM, Morrison TE, Vermeulen R, Aguirre-Ghiso JA, Rincon M and DeGregori J. Respiratory viral infections awaken metastatic breast cancer cells in lungs. Nature 2025; 645: 496-506.
[31] Guo M, Cai C, Zhao G, Qiu X, Zhao H, Ma Q, Tian L, Li X, Hu Y, Liao B, Ma B and Fan Q. Hypoxia promotes migration and induces CXCR4 expression via HIF-1α activation in human osteosarcoma. PLoS One 2014; 9: e90518.
[32] Thiery JP, Acloque H, Huang RY and Nieto MA. Epithelial-mesenchymal transitions in development and disease. Cell 2009; 139: 871-890.
[33] Pouysségur J, Dayan F and Mazure NM. Hypoxia signalling in cancer and approaches to enforce tumour regression. Nature 2006; 441: 437-443.
[34] Suzuki-Karasaki M, Ochiai Y, Innami S, Okajima H, Suzuki-Karasaki M, Nakayama H and Suzuki-Karasaki Y. Ozone mediates the anticancer effect of air plasma by triggering oxidative cell death caused by H_2O_2 and iron. Eur J Cell Biol 2023; 102: 151346.
[35] Liu YH, Wu LH, Fan WJ, Chiu SH, Chen PH, Wang CC and Lee CH. A tellurium-based small compound ameliorates tumor metastasis by downregulating heparanase expression. J Cancer 2024; 15: 5308-5317.

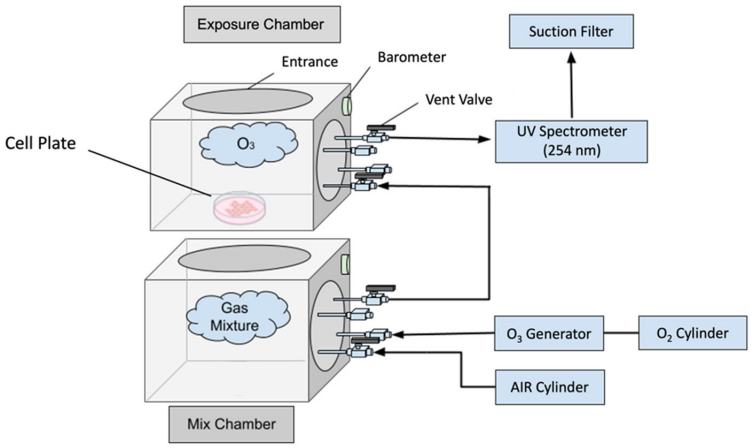

Supplementary Figure 1. Design of the ozone exposure system.

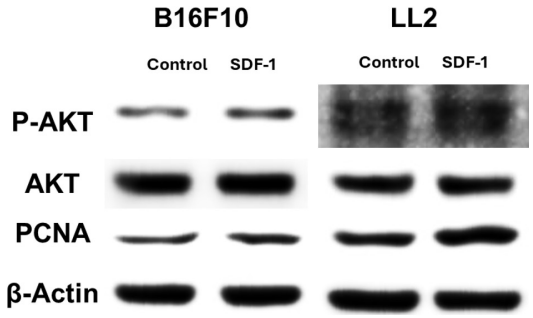

Supplementary Figure 2. P-AKT and PCNA expression were detected in B16F10 and LL2 cells by immunoblot analysis after exposure to SDF-1 (100 ng/ml) for 16 hours. The expression of β-actin served as the quantitative control.

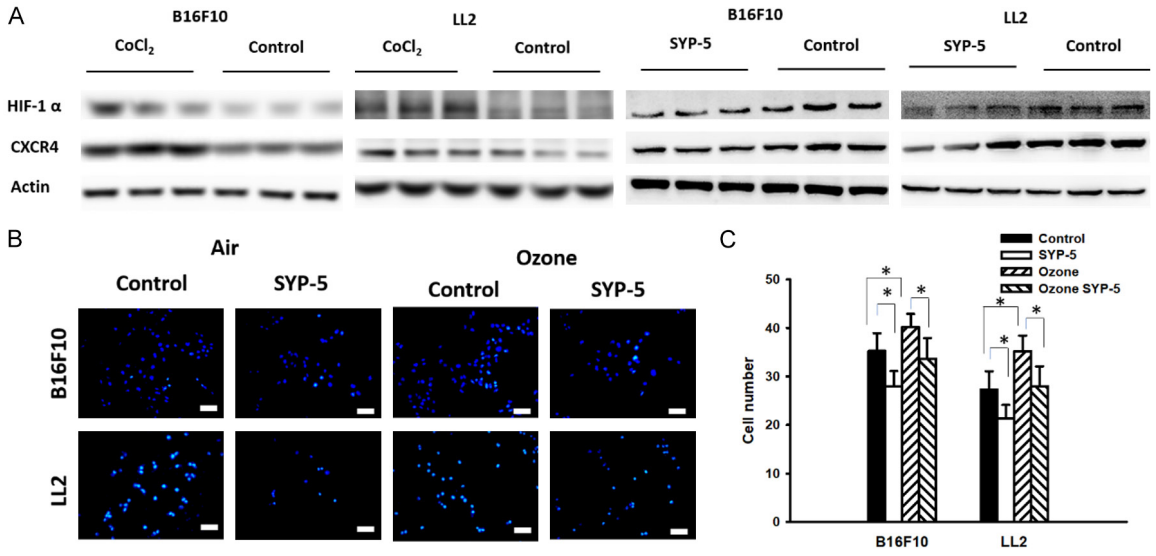

Supplementary Figure 3. (A) HIF-1α and CXCR4 expression were detected in B16F10 and LL2 cells by immunoblot analysis after exposure to $CoCl_2$ (200 μM) or SYP-5 (20 μM) for 16 hours. The expression of β-actin served as the quantitative control. B16F10 and LL2 cells were placed on the upper layer of Transwell and then treated with ozone or SYP-5 (20 μM). (B) The lower layer of Transwell was stained with DAPI, and (C) B16F10 and LL2 cells were counted using a fluorescence microscope 24 hours after exposure began (n = 6; mean ± SD; *P < 0.05). Scale bar = 50 μm (×200).